Available online at www.sciencedirect.com
SCIENCE DIRECT®
Journal of Catalysis 227 (2004) 117–129
JOURNAL OF CATALYSIS
www.elsevier.com/locate/jcat

Novel derivatives of MCM-36 as catalysts for the reduction of nitrogen oxides from FCC regenerator flue gas streams

Jan-Olaf Barth [a], Andreas Jentys [a], Eleni F. Iliopoulou [b], Iacovos A. Vasalos [b], Johannes A. Lercher [a,*]

[a] *Technische Universität München, Lehrstuhl II für Technische Chemie, 85747 Garching bei München, Germany*
[b] *Center for Research and Technology Hellas, Chemical Process Engineering Research Institute, PO Box 1517, 54006 University City, Thessaloniki, Greece*

Received 18 March 2004; revised 23 June 2004; accepted 24 June 2004
Available online 5 August 2004

Abstract

MCM-36 materials containing mixed oxide pillars ($MgO–Al_2O_3$-MCM-36, $BaO–Al_2O_3$-MCM-36, $MgO–Al_2O_3–SiO_2$-MCM-36, $BaO–Al_2O_3–SiO_2$-MCM-36) were investigated as additives for the in situ reduction of NO_x formed during the regeneration of coked cracking catalysts in FCC units. The additives were investigated under reaction conditions similar to the oxygen-depleted and the oxygen-enriched zone of the FCC regenerator. MCM-36-type materials with basic mixed oxide clusters in the interlayer galleries showed high NO conversions (∼ 85%) and high N_2 yields (∼ 80%) under oxygen-deficient reaction conditions. The catalytic activity of MCM-36 with alkaline earth metal aluminum oxide pillars incorporated between the zeolitic layers was higher ($MgO–Al_2O_3$-MCM-36: 77% N_2 yield at 650 °C) compared to the nonpillared parent material MCM-22 (22%). The materials have been added in regeneration experiments to industrial (coked) FCC catalysts in a fluidized-bed reactor. The materials led to a reduction of NO emissions also in the presence of Pt-based CO combustion promoters (∼ 30% NO reduction). It is speculated that Brønsted acid sites in the zeolite layers of the composite materials catalyze the reduction of NO with NH_3, which is an intermediate in the regeneration of nitrogen-containing carbonaceous deposits on deactivated FCC catalysts.

Keywords: Fluid catalytic cracking (FCC); NO_x reduction; Oxidative regeneration; Pillared zeolites

1. Introduction

Fluid catalytic cracking (FCC) is one of the largest applications of heterogeneous catalysis and is a key process in a modern refinery. Gasoline from FCC units contributes to approximately 35% of the US gasoline pool [1]. The production of petrochemical-based chemicals from FCC and related processes such as DCC (deep catalytic cracking) and CPP (catalytic pyrolysis process) is gaining increasing importance due to the worldwide shortage in production capacities for lower olefins [2]. Worldwide more than 300 FCC units are operated, converting vacuum gas oil and high boiling residues, primarily in the 315–650 °C boiling point range, into lighter fuel products and petrochemical feedstocks [3,4]. The FCC process consists of a riser reactor and a regenerator in which the deactivated cracking catalyst is regenerated by burning off the coke deposited on the FCC catalyst during the catalytic cracking reaction. The high-temperature flue gas stream at the exit of a regenerator contains O_2, N_2, CO, CO_2, H_2O, SO_x, and NO_x. Depending upon feed nitrogen levels and regenerator conditions NO_x concentrations are typically in the range of 50–500 ppm [5,6]. The NO_x emissions from the regenerator of a FCC can contribute up to 50% of the total NO_x emissions in a refinery and consist mainly of NO, which is formed in the regenerator, while NO_2 is formed only after NO is being released to the air. N_2O in the exit gas of an FCC regenerator, if any, exists typically in very low concentrations [7]. NO is formed in the

* Corresponding author. Fax: +49/89/28913544.
E-mail address: johannes.lercher@ch.tum.de (J.A. Lercher).

0021-9517/$ – see front matter
doi:10.1016/j.jcat.2004.06.021

FCC process by the oxidation of nitrogen-containing compounds in coke (fuel NO_x) [5,6,8], while the reaction of air-derived nitrogen and oxygen produces negligible amounts of NO (thermal NO_x).

Regulations that confine the emissions of nitrogen oxides (NO_x) from the regenerator of a FCC unit are becoming more and more stringent due to environmental concerns and to the use of heavier feedstocks [1,3]. NO_x control technologies for the FCC unit should reduce NO emissions without adversely affecting the cracking activity and selectivity of the FCC catalyst or increasing the emissions of other pollutants. Current NO_x control strategies include (see Ref. [9] and references therein) (i) hydrotreating of the feed to minimize NO_x precursors (polycyclic aromatic hydrocarbons of carbazole or pyridine type) in the FCC unit, (ii) flue gas treatment in a tail-end unit with either NH_3 or hydrocarbon injection [10], and (iii) modification of the design or the operating conditions of the regenerator, as, e.g., the development of a countercurrent regenerator or a two-stage regenerator. Other modifications of the FCC are the addition of a vaporizable fuel to the upper portion of the FCC regenerator, or the utilization of a spent catalyst distributor in the regenerator, and (iv) the use of catalytic additives, which is a simple, cost-effective method that is applicable in existing FCC units without significant modifications in the regenerator design or the unit operating conditions. These additives should operate at high temperatures and in the presence of other gases such as CO, CO_2, O_2, and H_2O. Materials that reduce NO_x emissions under the conditions of the regenerator of a FCC unit have been previously patented and/or reported by several research groups [3,6,9,11–13]. Typically, most of the modern refineries add CO combustion promoters (Pt-based compounds that accelerate the oxidation of CO) into their FCC catalyst inventories. However, CO combustion promoters increase NO emissions through the oxidation of nitrogen-containing intermediates such as HCN and NH_3 [5,6,8,14,15]. Aiming at the reduction of NO emissions several methods have been proposed, such as steam treating of conventional CO combustion promoters [3,16].

Consequently, there is an urgent need for the development of catalytic NO_x reduction additives that can either operate in the presence of a CO combustion promoter or have the ability to simultaneously reduce NO and CO emissions. In this contribution we discuss the use of novel derivatives of the molecular sieve MCM-36 as catalytic additives for the reduction of NO from FCC regenerator flue gas streams. These materials are characterized by a nanocomposite structure consisting of layers of zeolite MCM-22 (MWW type) and intercalated mixed oxides such as $MgO–Al_2O_3$, $BaO–Al_2O_3$, $MgO–Al_2O_3–SiO_2$, and $BaO–Al_2O_3–SiO_2$ [17–21]. Mixed oxides and spinel-type materials containing MgO and BaO function as effective catalysts for the decomposition of NO at high temperatures ($> 500\,^{\circ}C$) and are used as SO_x transfer reagents for the reduction of SO_x emissions from FCC units [3,22]. Exfoliation of the zeolite layers of the uncalcined precursor of MCM-22 and intercalation of various (aluminum) oxides leads to derivatives of MCM-36 with particular physicochemical properties [23]. These nanocomposite materials are characterized by zeolitic microporosity in the zeolite phases and mesoporosity in the pores and galleries generated by oxide clusters in the interlayer space. In addition, the modular structure of the materials consists of the microporous zeolite phases containing Lewis- and Brønsted-type acid sites, which can be modified by ion exchange [24]. As the incorporated mixed oxides show basic properties bifunctional catalyst can be created [23]. Compared with other mesoporous materials such as MCM-41-type materials, materials based on MCM-36 are characterized by a much stronger acidity [17,19].

The scope of this work was to study the catalytic performance of NO_x reduction additives based on MCM-36 under reaction conditions that reproduce those in the regenerator of a typical FCC unit. The catalysts were investigated under reaction conditions simulating the oxygen-depleted and the oxygen-rich zone of an FCC regenerator operating under full burn conditions. Oxygen-deficient reaction conditions are encountered in the oxygen-depleted zones of the dense and the diluted phase of the FCC fluidized bed. The incomplete combustion of coke leads to the formation of a reductive atmosphere in parts of the dense phase of the fluidized bed mainly due to the formation of CO and some hydrocarbons not desorbed in the stripper [25–27]. Simultaneously, in the bottom region of the regenerator near the air inlet an oxygen-rich zone is encountered. The MCM-36-type materials were tested as catalysts for the reduction of NO with CO as well as in regeneration experiments mixed with spent FCC catalysts in a fluidized-bed reactor. The compatibility of the additives with a conventional Pt-based CO combustion promoter was also investigated. The reaction mechanism that leads to the reduction of NO by CO to N_2 was studied by IR spectroscopy.

2. Experimental

2.1. Synthesis of catalytic additives

Nanocomposite materials based on MCM-22 were synthesized according to the procedure described in Ref. [21]. All catalytic additives were thoroughly characterized and identified as derivatives of MCM-36 as described in Ref. [23].

2.2. Coked FCC catalysts

Coked (spent) FCC catalysts were obtained from an FCC unit using no CO combustion promoter (elemental analysis C, 1.31 wt%; H, 0.055 wt%; N, 233 ppm). The deactivated catalyst samples were extracted from a DCR (Davison circulating riser) unit after steam stripping.

2.3. Catalytic measurements

The catalytic activity of the samples was studied in a continuous flow system using a fixed-bed quartz reactor of 4 mm inner diameter containing 0.1 g of catalyst (particle size 300 µm). The reactant gas consisted of either 1000 ppm NO, 5% CO, and 2.5% O_2 or 600 ppm NO, 1.4% CO, and 0.7% O_2 while in both cases He was used as the carrier gas. A total flow of 100 ml/min resulting in a space velocity of 38,000 h^{-1} was used. The reaction products were analyzed with a chemiluminescence analyzer (NO–NO_2 analysis, Thermo Environmental Instruments, TEI-42-C) and a gas chromatograph (HP) equipped with a TCD detector. A MS 5A column was used for the separation of N_2, O_2, and CO and a Porapack Q column for N_2O and CO_2 partition. Before the reaction, the catalysts were activated in He flow at 600 °C for 1 h. Kinetic measurements were carried out at temperature intervals of 25 °C between 500 and 750 °C. The catalysts were equilibrated at each temperature for 165 min.

2.4. FCC regeneration experiments

Regeneration experiments were carried out in a bench-scale reaction unit using a protocol that simulates the regenerator of a typical fluid catalytic cracking unit [28]. The unit consists of the feed gas system, a fluidized-bed reactor, a furnace, and the gas analysis system. A detailed description of this unit can be found in Ref. [28]. The total flow rate was 1000 ml/min. The feed composition was 2% O_2 in N_2. Mechanical mixtures of spent catalyst (from a commercial FCC unit using no CO combustion promoter) with 1 wt% of candidate additives were loaded in the reactor and regeneration was carried out at 700 °C. The total reactor loading was 10 g in all experiments. To investigate the compatibility of the additives with conventional Pt-based CO combustion promoters the regeneration experiments were repeated loading the reactor with mechanical mixtures of 1 wt% of the candidate additives, 0.1 wt% of CP-3, a commercial CO promoter supplied by Grace-Davison, and 98.9 wt% spent catalyst.

2.5. IR spectroscopy

IR measurements were performed with a Bruker IFS-88 spectrometer in an in situ flow cell. The spectrometer was used in the transmission-absorption mode with a resolution of 4 cm^{-1}. The IR cell consisted of a stainless-steel chamber equipped with CaF_2 windows and a resistance-heated furnace in which the samples pressed into thin, self-supporting wafers of approximately 5 mg/cm^2 were placed. The samples were activated in situ in a flow of He at 450 °C (heating rate 10 °C/min) for 60 min. After activation, the system was cooled to the adsorption temperature (200 °C). The amounts of 1000 ppm NO in He, 1000 ppm NO + 3% O_2 in He, and 5% CO in He were adsorbed at 200 °C in successive adsorption steps.

2.6. Temperature-programmed desorption (TPD) of NO_2

Temperature-programmed desorption of NO_2 was used for the investigation of surface species such as nitrates and nitrites on the samples. The sample (∼ 100 mg) was degassed by evacuation to 10^{-3} mbar, followed by heating at a rate of 10 °C/min to 450 °C and maintaining at that temperature for 60 min. After cooling to 100 °C, the sample was equilibrated with 10 mbar of 1% NO_2 in He for 60 min. Subsequently, the system was evacuated to 10^{-3} mbar for 180 min and heated to 600 °C at a rate of 10 °C/min. During the temperature ramp, mass spectra of the gas phase were collected at 5 °C/min intervals using a Balzers QMG 420 mass spectrometer to determine the rate of desorption.

3. Results

3.1. Materials

Table 1 summarizes the textural properties and the concentrations of the acid sites (determined from temperature-programmed desorption of ammonia [23]) of the derivatives of MCM-36 investigated. A detailed physicochemical characterization and investigation of the acid–base character of the nanocomposite materials can be found in Refs. [21] and [23].

3.2. Kinetic measurements

All materials were tested as catalysts for the reduction of NO with CO under reaction conditions simulating the FCC regeneration process. CO is the dominating reducing agent in the regenerator, due to the incomplete combustion of coke. Fig. 1 shows an example for the reduction of NO with CO over MgO–Al_2O_3-MCM-36 under conditions similar to the oxygen-depleted (Fig. 1a) and oxygen-rich (Fig. 1b) phase of an FCC regenerator operated under full burn conditions. N_2, NO_2, and N_2O were formed as reaction products, while CO_2 was generated by the subsequent oxidation of CO. In the temperature region between 600 and 750 °C high yields (50–84%) of N_2 were obtained under reaction conditions similar to the oxygen-depleted dense and diluted phases of the fluidized bed of the FCC regenerator (0.5% O_2). In the presence of higher oxygen concentrations (2.4% O_2), which are encountered in the lower parts of the dense phase, significantly lower yields (10–40%) of N_2 were measured. In the first case considerable amounts of N_2O were formed with a maximum yield of 50% at 575 °C, whereas under the reaction conditions with high oxygen concentration only 17% N_2O was formed with its maximum shifted to higher temperatures (625 °C). In contrast to this observation, under oxygen-rich conditions (2.4% O_2) higher yields of NO_2 were obtained. For both cases the conversion of CO and yield of CO_2 increased with rising temperature and reached a constant maximum degree of conversion at 575–600 °C.

Table 1
Elemental composition, BET surface areas, and acid site concentrations (determined from temperature-programmed desorption of NH_3) of derivatives of MCM-36 and the MCM-22 parent material

Sample	Si (wt%)	Al (wt%)	Na (wt%)	Mg (wt%)	Ba (wt%)	S_{BET} (m^2/g)	$c_{acid\ sites}$ (mmol/g)
MCM-22	45.40	3.85	0.25	–	–	432	0.79
$MgO–Al_2O_3$-MCM-36	27.92	21.28	< 0.10	0.64	–	348	0.91
$BaO–Al_2O_3$-MCM-36	9.33	35.90	< 0.10	–	2.20	390	0.31
$MgO–Al_2O_3–SiO_2$-MCM-36	39.90	4.32	< 0.10	0.24	–	757	0.42
$BaO–Al_2O_3–SiO_2$-MCM-36	40.06	4.48	< 0.10	–	0.24	689	0.38

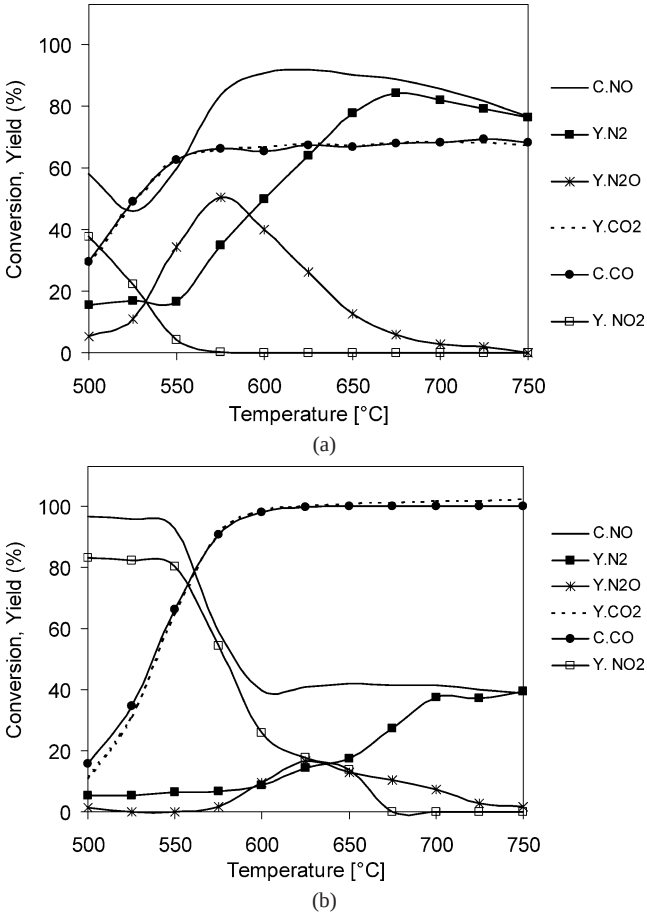

Fig. 1. NO reduction with CO over $MgO–Al_2O_3$-MCM-36: (a) 700 ppm NO, 1.4% CO, 0.5% O_2, (b) 1000 ppm NO, 4.4% CO, 2.4% O_2.

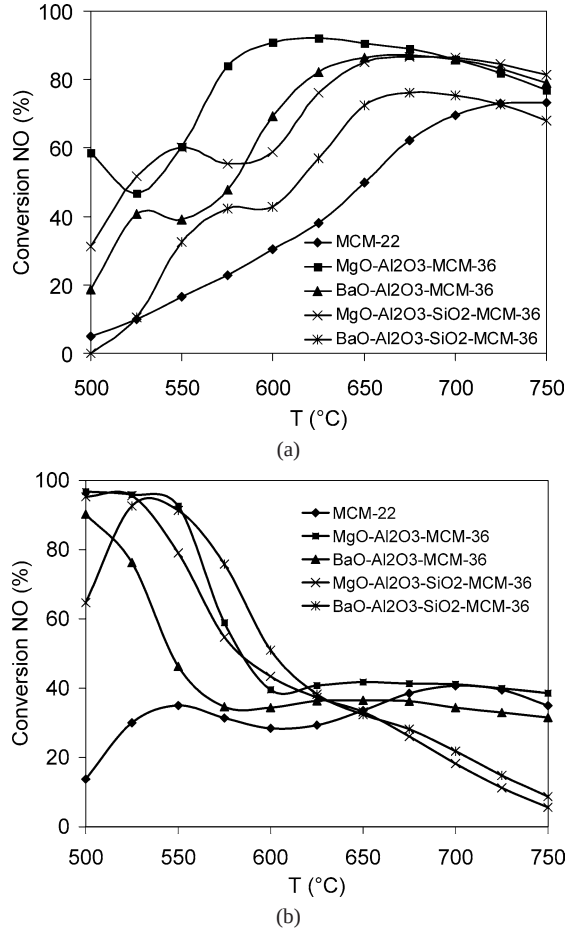

Fig. 2. NO conversion over MCM-22 and derivatives of MCM-36: (a) 700 ppm NO, 1.4% CO, 0.5% O_2, (b) 1000 ppm NO, 4.4% CO, 2.4% O_2.

The comparison of the conversion of NO in the reaction with CO over various MCM-36 derivatives and the precursor material zeolite MCM-22 is shown in Fig. 2. Highest conversions of NO (∼ 90%) were obtained for $MgO–Al_2O_3$-MCM-36 and $BaO–Al_2O_3$-MCM-36 in the presence of lower oxygen concentrations (Fig. 2a). Under conditions simulating the oxygen-rich phase of the regenerator (Fig. 2b) $MgO–Al_2O_3$-MCM-36, $BaO–Al_2O_3$-MCM-36, and MCM-22 reach similar degrees of conversion (32–40%) in the range of 675–750 °C, while for $MgO–Al_2O_3–SiO_2$-MCM-36 and $BaO–Al_2O_3–SiO_2$-MCM-36 the conversion of NO decreased with increasing temperature. The high conversions of NO over the mixed oxide intercalated nanocomposite materials in the region of 500–600 °C is mainly due to the formation of NO_2.

The yields of N_2 formation as a function of temperature over MCM-36 derivatives and MCM-22 are shown in Fig. 3. Under oxygen deficient conditions the yields of N_2 increased with increasing temperature. The highest yields of N_2 (75–83%) were obtained for $MgO–Al_2O_3–SiO_2$-MCM-36 and $MgO–Al_2O_3$-MCM-36, whereas for MCM-22 and $BaO–Al_2O_3–SiO_2$-MCM-36 the lowest yields of N_2 were obtained in the temperature window characteristic of the FCC regenerator (600–750 °C). In the presence of an excess of oxygen (Fig. 3b) generally lower yields of N_2 were observed with a maximum of 40% for $MgO–Al_2O_3$-MCM-36.

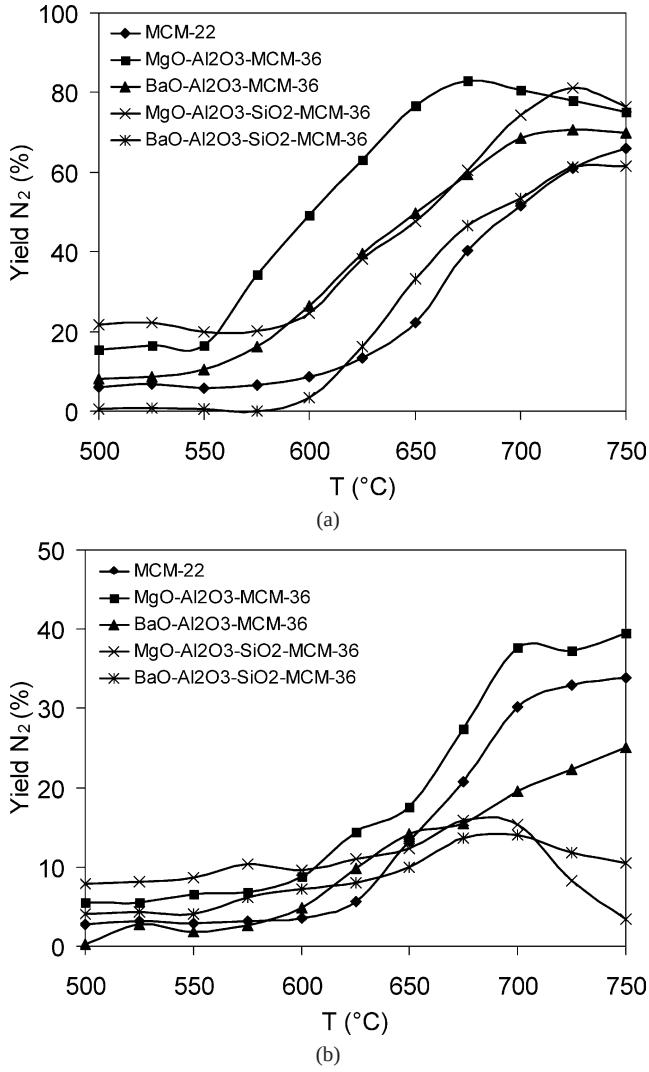

Fig. 3. Yield of N_2 over MCM-22 and derivatives of MCM-36: (a) 700 ppm NO, 1.4% CO, 0.5% O_2, (b) 1000 ppm NO, 4.4% CO, 2.4% O_2.

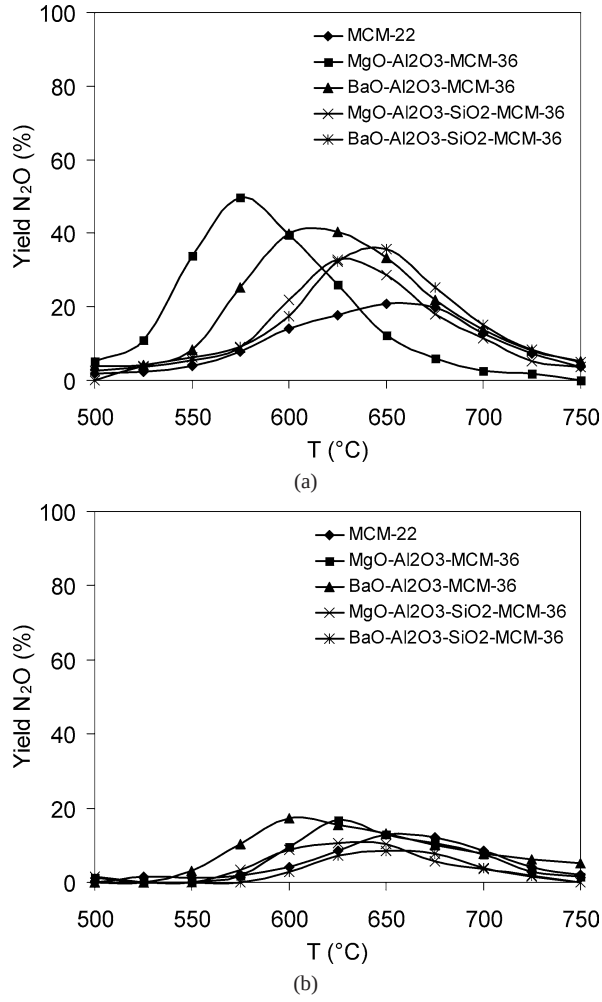

Fig. 4. Yield of N_2O over MCM-22 and derivatives of MCM-36: (a) 700 ppm NO, 1.4% CO, 0.5% O_2, (b) 1000 ppm NO, 4.4% CO, 2.4% O_2.

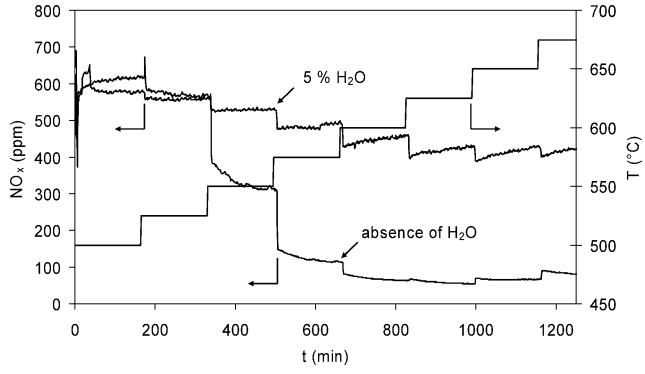

Fig. 5. Time-on-stream measurement of the reaction of NO with CO over MgO–Al_2O_3-MCM-36 in the absence or presence of 5% H_2O (initial concentrations of reactants: 690 ppm NO, 1.4% CO, 0.5% O_2).

Interestingly, MCM-22 showed higher yields in the range of 650–750 °C (34% at 750 °C) compared to the three other MCM-36 derivatives. Highest selectivities to N_2 were obtained for MgO–Al_2O_3-MCM-36 (94% selectivity at 86% NO conversion, 700 °C) and MgO–Al_2O_3–SiO_2-MCM-36 (86% selectivity at 86% NO conversion, 700 °C), while the BaO containing pillared zeolites and the nonpillared parent material MCM-22 showed lower selectivities (71–80%).

As already pointed out N_2O is one of the by-products in the reaction of NO with CO over MCM-36 type catalysts. Fig. 4 shows the yield of N_2O as a function of temperature under the two different reaction conditions. Lower oxygen concentrations (0.5 vs 2.4%) favored higher yields of N_2O. The highest yield of N_2O (∼ 50%) was detected at 575 °C for MgO–Al_2O_3-MCM-36 followed by BaO–Al_2O_3-MCM-36 (∼ 40%, 610 °C). Note that for BaO–Al_2O_3–SiO_2-MCM-36 the maximum of N_2O formation was found at higher temperatures than for MgO-containing MCM-36 derivatives with SiO_2/Al_2O_3 pillars (650 vs 625 °C). Under oxygen-deficient conditions the lowest yields of N_2O were obtained for the unmodified MCM-22 zeolite (21%, 650 °C). In the presence of higher oxygen concentrations similar yields of N_2O were obtained for BaO–Al_2O_3-MCM-

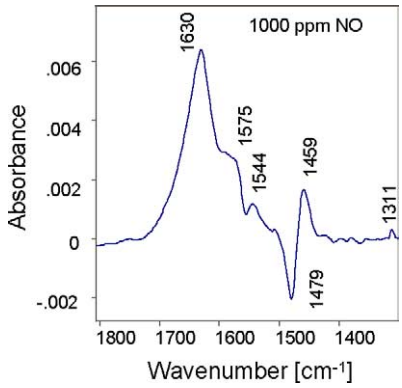

Fig. 6. Difference of IR spectra measured after adsorption of 1000 ppm NO on MgO–Al_2O_3-MCM-36 ($T = 200\,^{\circ}C$).

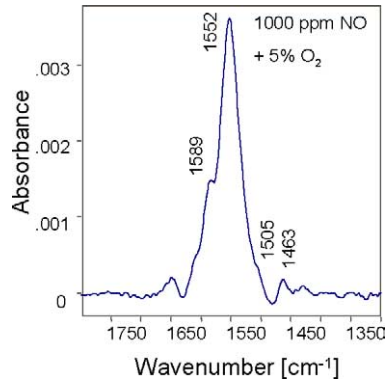

Fig. 7. Difference of IR spectra measured after adsorption of 1000 ppm NO and 5% O_2 on MgO–Al_2O_3-MCM-36 ($T = 200\,^{\circ}C$).

36 and its MgO derivative ($\sim 17\%$), while the lowest yields were determined for the SiO_2-modified materials.

Fig. 5 shows the time-on-stream behavior of MgO–Al_2O_3-MCM-36 compared in the absence and presence of 5% water over 20 h at 500–675 °C. To investigate the detrimental effects of water (steam) on the catalyst the temperature was increased by steps of 25 °C and the catalysts were maintained at each temperature for 165 min. Under water-free conditions the pillared zeolites showed stable catalytic activity, while in the presence of 5% water the catalytic activity decreased after ~ 5.5 h at 550 °C with duration of the experiment and significantly lower conversions of NO ($\sim 34\%$ at 675 °C) were observed.

3.3. IR spectroscopy: Adsorption of NO, O_2, and CO on MgO–Al_2O_3-MCM-36

To investigate the intermediate species formed on the surface during the reduction of NO with CO in the presence of oxygen NO and O_2 were coadsorbed followed by adsorption of CO. The differences in the IR spectra obtained after adsorption of 1000 ppm NO on MgO–Al_2O_3-MCM-36 are shown in Fig. 6. The formation of nitrite and nitrate species (bridged bidentate nitrate, monodentate nitrate on Al, linear nitrite on Al) was observed (for an assignment of the band see Table 2) [29,30]. The decreasing band at 1479 cm^{-1} indicated that carbonates (resulting from the exposure of the sample to air) on the basic material were removed upon NO adsorption. Note that nitrates were formed, although the adsorption was carried out in the absence of oxygen.

After adsorption of 1000 ppm NO in the presence of 3% O_2 predominantly nitrate species were formed on the nanocomposite materials (Fig. 7). Bands at 1575 cm^{-1} characteristic of monodentate nitrates on Al and 1552 cm^{-1} (bidentate nitrate on Al close to Mg) were observed, whereas nitrites (1459, 1463 cm^{-1}: linear nitrite on Al) were only detected in minor concentrations under oxidative conditions.

After adsorption of NO and O_2 the sample was equilibrated with 5% CO in He. Fig. 8 shows differences in the IR spectra measured during heating of the catalyst from 200 to 500 °C in the presence of CO. Bands indicative of nitrates and nitrites decreased in intensity (negative bands), while bands at 1378, 1384 1588, 1610, and 1637 cm^{-1} first increased in intensity, reached a maximum at $\sim 350\,^{\circ}C$, and finally decreased with increasing temperature. Partially overlapping bands at $\sim$ 2280–2240 and 2227 cm^{-1} were observed above 250 °C, which increased in intensity with increasing temperature. These IR bands can be attributed to bicarbonate (1445, 1646 cm^{-1}, shoulder at 3610 cm^{-1}), uni-(1410, 1540–1580 cm^{-1}) and bidentate (1378 cm^{-1}) carbonate species adsorbed on basic sites of the MgO–Al_2O_3-MCM-36 material. Bands at 2930 (not shown) 1610

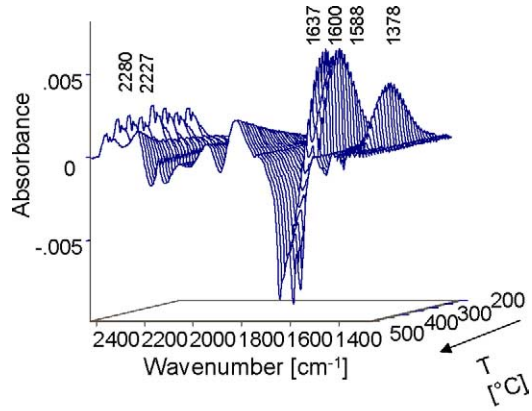

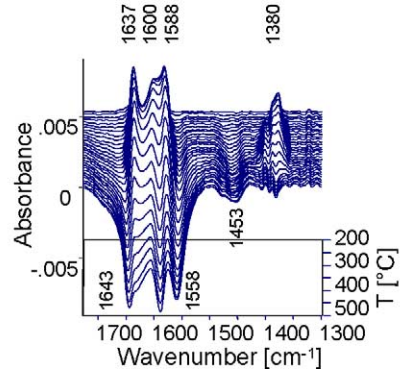

Fig. 8. Differences of IR spectra measured during reaction of 5% CO on MgO–Al_2O_3-MCM-36 after exposure of the catalyst to 1000 ppm NO and 5% O_2 ($T = 200\,^{\circ}C$).

Table 2
Assignment of IR bands for species on $MgO–Al_2O_3$-MCM-36

Species	Structure	Remarks	Position /(cm^{-1})
Bridged bidentate nitrate	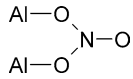		1630
Monodentate nitrate	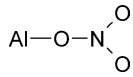	High coverage	1588
		Low coverage	1575
Bidentate nitrate on Al close to Mg	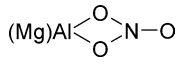		1552
Linear nitrite on Al	Al–O–N–O		1459
Bicarbonate	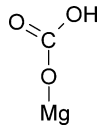		1445, 1646
Unidentate carbonate	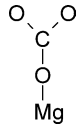		1410, 1479
Bidentate carbonate	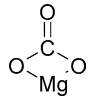		1378
Isocyanates	Mg–N=C=O Al–N=C=O		2240 2260
N_2O			2227
Formate	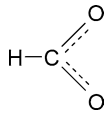	ν (sym) ν (asym) δ (CH)	2930 1610 1384

and 1384 cm^{-1} indicated the presence of formate species on the $MgO–Al_2O_3$ clusters [31]. The broad bands around 2280–2240 cm^{-1} are indicative of the degenerate stretching vibration of surface isocyanate species adsorbed on the $MgO–Al_2O_3$ pillars (Al–NCO, 2260; Mg–NCO, 2240 cm^{-1}) [29,32]. The narrow peak centered at 2227 cm^{-1} is tentatively ascribed to the N–N stretching vibration of N_2O formed during the reaction [29].

During reaction of CO on the catalyst at 500 °C nitrate and nitrite bands continued to decrease (negative bands in Figs. 8 and 9) accompanied by increasing intensities of the peaks characteristic of isocyanate species (2260 cm^{-1}) and N_2O (2227 cm^{-1}).

3.4. Temperature-programmed desorption of NO_2

NO_2 was adsorbed on $MgO–Al_2O_3$-MCM-36 to study the thermal stability of nitrate surface species formed on the catalysts. The samples were exposed to NO_2 to simulate the interaction with NO_x species under oxidative conditions. The temperature-programmed desorption of NO_2 (fragment NO: $m/e = 30$) from $MgO–Al_2O_3$-MCM-36 and from the nonpillared parent material MCM-22 is compared in Fig. 10. In comparison with MCM-22, significantly more NO_2 was adsorbed on the basic oxide pillars of the composite material. The first maximum of desorption at ∼ 200 °C is tentatively assigned to the desorption of physisorbed NO_2, while the maximum at 310 °C and the less intense maxima at 440 and 510 °C are tentatively attributed to the decomposition of monodentate and (bridged) bidentate nitrate species. Interestingly, some nitrate species decompose in vacuum (the TPD experiment was performed at a base pressure of 10^{-3} mbar) at elevated temperatures above 500 °C, suggesting the presence of nitrates with a high thermal stability.

3.5. FCC regeneration experiments

To evaluate the behavior of the MCM-36-type additives during the regeneration process of the FCC catalysts, 1 wt% of nanocomposite material was added to a coked cracking catalyst from an industrial FCC unit and regenerated at 700 °C with 2% O_2 in a fluidized-bed reactor. These conditions were selected to represent a full-burn regenerator operation [28]. During regeneration NO was formed from

Table 3
Conversion of NO and CO during the oxidative regeneration of a coked FCC catalyst in a fluidized-bed reactor in the presence of 1 wt% of MCM-36-type catalysts or a conventional Pt-based CO combustion promoter (CP-3). Using CP-3 the amount of NO released increased by −300%

Sample	NO conversion as compared to pure spent catalyst (%)	CO conversion as compared to pure spent catalyst (%)
$MgO–Al_2O_3$-MCM-36	14	5
$BaO–Al_2O_3$-MCM-36	21	2
$MgO–Al_2O_3–SiO_2$-MCM-36	12	3
$BaO–Al_2O_3–SiO_2$-MCM-36	18	1
CP-3	−300	86

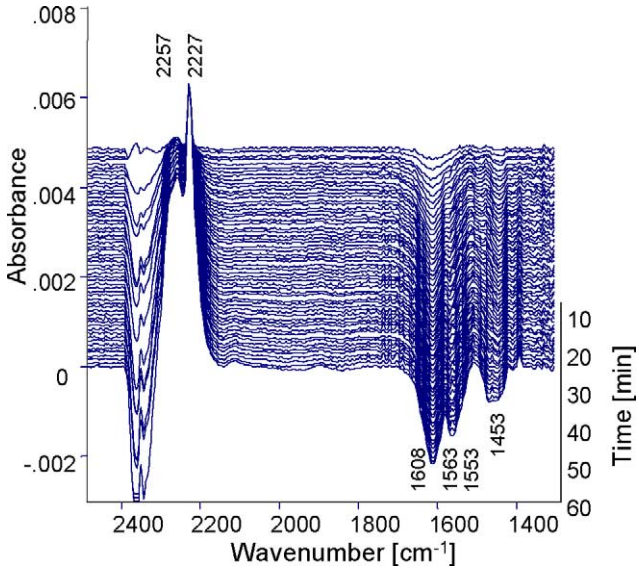

Fig. 9. Differences of IR spectra measured during reaction of 5% CO on $MgO–Al_2O_3$-MCM-36 after exposure of the catalyst to 1000 ppm NO and 5% O_2 ($T = 500\,^{\circ}C$).

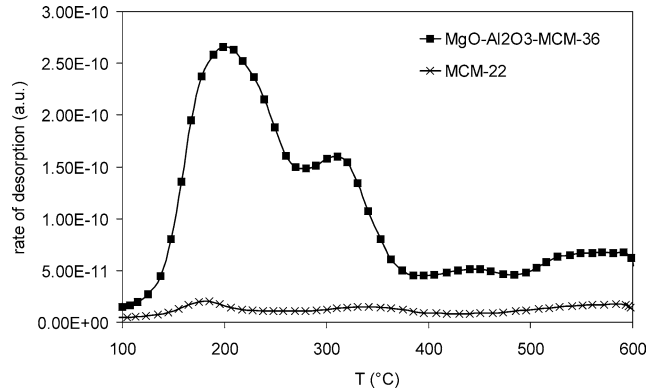

Fig. 10. Temperature-programmed desorption of NO_2 (fragment NO, $m/e = 30$) from $MgO–Al_2O_3$-MCM-36 and MCM-22.

oxidation of the nitrogen-containing species of the spent catalyst. Table 3 provides a comparison of the reduction of NO in the presence of the various additives or a conventional Pt-based CO combustion promoter (CP-3). Compared to spent catalyst only (base case) all materials, except CP-3, showed a reduction of NO emissions. Best results (18–21% NO conversion) were achieved for $BaO–Al_2O_3$-MCM-36 and $BaO–Al_2O_3–SiO_2$-MCM-36, whereas for the MCM-36-type derivatives containing MgO only 12–14% conversion was obtained. However, all composite materials showed a reduction of NO emissions, while CP-3 led to significant increase in NO emissions by ∼ 300%. In contrast to the Pt-based CO combustion promoter, the MCM-36-type materials facilitated only very small conversions of CO to CO_2. The comparison of the evolution of CO and NO emissions during the regeneration experiment in the fluidized-bed reactor for the base case (absence of any additive) and in the presence of 1 wt% $BaO–Al_2O_3$-MCM-36 added to the coked cracking catalyst is shown in Fig. 11. For the base case, the majority of CO was released in the first 8 min of the experiment, while a significantly smaller amount was determined in the following 35 min with a second maximum after 18 min. Interestingly, the formation of NO was observed in parallel to this second CO evolution with a maximum 18–20 min after the start of the experiment. Only when the maximum CO concentration diminished, the coke nitrogen was converted to NO. Dishman et al. measured the concentration profile of combustion gases during regeneration and observed a similar behavior [33]. In the presence of $BaO–Al_2O_3$-MCM-36 21% less NO was released and nearly all CO was consumed in the region of the second CO maximum of the base case, while only very little effect on CO formation was observed in the first 10 min of the experiment. Similar observations were made for all other MCM-36-type additive investigated in this study.

In most of the industrial FCC regeneration units operating under full-burn conditions the CO emissions are commonly controlled by using Pt-based CO combustion promoters in the FCC catalyst inventories. As pointed out such additives might cause a significant increase of the NO emissions. Therefore, we have tested the compatibility of our catalysts with a commercial CO promoter (CP-3) to achieve a simultaneous reduction of CO *and* NO emissions in a experiment in which the spent catalyst was mixed with 0.1 wt% CP-3 and the regeneration was carried out under the same conditions (700 °C, 2% O_2 in N_2). Table 4 exemplifies the performance of the additives in the presence of 0.1 wt% CP-3. A reduction of CO emissions by 51–86% compared to the base case (pure spent catalyst) was achieved. In the presence of the MCM-36-type derivatives less NO was released compared to the experiment with CP-3 only. Best results were obtained for $BaO–Al_2O_3–SiO_2$-MCM-36, which lowered the NO emissions by 31% compared to the Pt-based CO combustion promoter. However, the additive also led to a decrease of CO

Table 4
Conversion of NO and CO during the regeneration of a coked FCC catalyst in a fluidized-bed reactor in the presence of 1 wt% of MCM-36-type catalysts *and* 0.1 wt% of a conventional Pt-based CO combustion promoter (CP-3)

Sample	CO conversion as compared to pure spent catalyst (%)	NO conversion as compared to regeneration in the presence of CP-3 (%)
CP-3	86	–
$MgO–Al_2O_3$-MCM-36/CP-3	86	6
$BaO–Al_2O_3$-MCM-36/CP-3	69	16
$MgO–Al_2O_3–SiO_2$-MCM-36/CP-3	57	23
$BaO–Al_2O_3–SiO_2$-MCM-36/CP-3	51	31

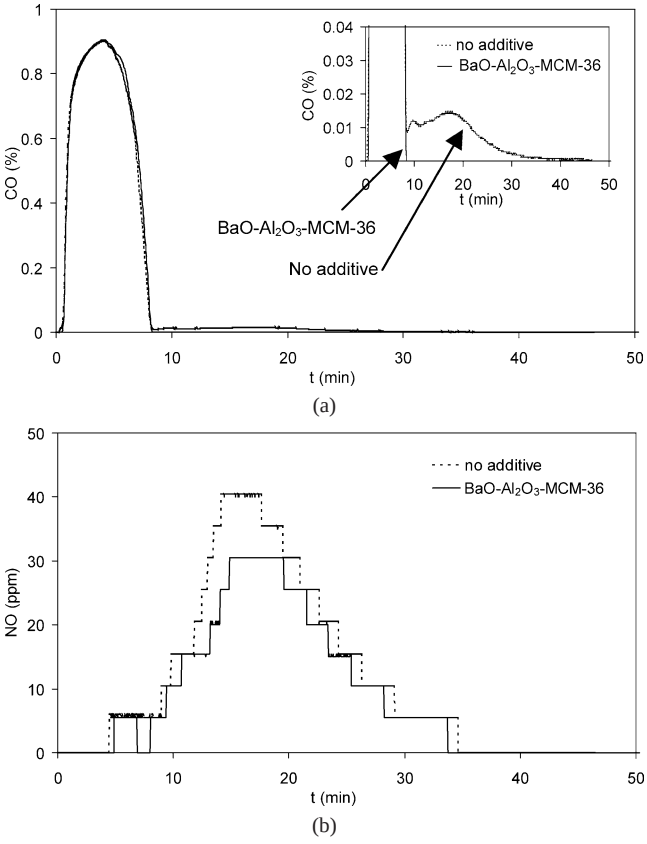

Fig. 11. Formation of (a) CO and (b) NO during the oxidative regeneration (2% O_2) of a spent FCC catalyst in the absence or presence of 1 wt% $BaO–Al_2O_3$-MCM-36 in a fluidized bed reactor.

conversion to ∼ 51% compared to 86% in the sole presence of CP-3.

4. Discussion

4.1. Reaction mechanism

The results demonstrate the high catalytic activity of MCM-36-type materials containing mixed alkaline earth aluminum oxide pillars in the reduction of NO with CO to N_2 and CO_2, in the presence of oxygen. Generally, the conversion of NO and yields of N_2 and N_2O were significantly higher under oxygen-deficient reaction conditions, which are encountered in the oxygen-depleted zones of the dense and the diluted phase of the FCC regenerator. Higher oxygen concentrations inhibit the reduction of NO by CO, as the CO/O_2 reaction is favored at the expense of the CO/NO reaction [34,35]. Under reaction conditions similar to the oxygen-rich zone, which is encountered in the bottom region of the regenerator near the air grid (500–625 °C; oxygen excess), NO is mainly converted to NO_2 over the MCM-36 derivatives (see Fig. 1b). In comparison to zeolite MCM-22 ("parent material") an increase in the catalytic performance was observed when $MgO–Al_2O_3$ and $BaO–Al_2O_3$ oxide pillars were incorporated between the zeolitic layers, suggesting that the mixed oxide clusters are the catalytically active sites. The conversion of NO and yield to N_2 increased with increasing Mg and Ba concentrations in the additives. As a direct oxidation of NO to NO_2 is not favored thermodynamically at high temperatures, high yields to NO_2 can only be attributed to the decomposition of surface nitrite and nitrate species formed on the basic oxide clusters ($MgO–Al_2O_3$, $BaO–Al_2O_3$) in the interlayer galleries. The temperature-programmed desorption of NO_2 from $MgO–Al_2O_3$-MCM-36 (Fig. 10) has shown that such ionic NO_x species still decompose in the high-temperature region above 500 °C. The formation of surface nitrite and nitrate species (mono-, bidentate, bridged nitrates) was observed by IR spectroscopy on the basic MCM-36-type materials (cf. Figs. 6 and 7). The interaction of NO with the pillared zeolites led to the removal of carbonate species (negative band at 1479 cm^{-1} in Fig. 6) present on the basic oxide clusters and the formation of different ionic NO_x surface species, which are probably located on the pillars between the zeolite layers. Interestingly, nitrates were also formed in the absence of O_2, suggesting that an oxidation of NO by reactive oxygen species is present in the mixed oxide clusters in the interlayer galleries. In the presence of 3% O_2 mainly nitrate species were observed on the surface with bidentate nitrates on Al close to Mg (1552 cm^{-1}) being the dominant species.

The in situ IR experiments showed that with increasing temperature the presence of CO led to a removal of nitrite and nitrate species from the catalyst surface. Simultaneously, formate and various (bi-) carbonate species were observed, which can only result from an oxidation of CO during the reaction with the surface NO_x species. The concentration of carbonate and formate species adsorbed on basic sites reached a maximum at ∼ 350 °C, which can be explained by a thermal desorption of the weakly bound species. Note

that for $MgO–Al_2O_3$-MCM-36 and $BaO–Al_2O_3$-MCM-36 two types of basic hydroxyl groups were detected by CO_2 adsorption: (i) Mg(Ba)–OH and (ii) Al_{IV}–OH groups on the spinel-type oxide clusters [23,36]. The latter basic sites were attributed to hydroxyl groups on aluminum ions in a tetrahedral coordination sphere of the defect spinel-type oxide pillaring clusters.

For the understanding of the reaction mechanism of NO reduction with CO over the MCM-36-based catalysts the formation of isocyanate species and N_2O at temperatures above 300 °C is important. The partially overlapping IR bands at ~ 2260 and 2240 cm^{-1} (Al–NCO and Mg–NCO, respectively) indicated that the –NCO intermediates are most probably adsorbed on the $MgO–Al_2O_3$ pillars [29,32]. Simultaneously with the observation of isocyanate species the formation of N_2O was revealed by the intense band of the N_2O stretching vibration at 2227 cm^{-1}. Isocyanates such as Al–NCO and Mg–NCO species may be formed by the reaction of nitrite and nitrate species with CO. The formation of the N–N bond during the reduction of NO with CO leading to N_2 and N_2O, is tentatively ascribed to the reaction of surface isocyanates with NO:

$$\text{Al–NCO} + \text{NO} \rightarrow \text{N}_2 + \text{CO}_2, \tag{1}$$

$$\text{Al–NCO} + \text{NO} \rightarrow \text{N}_2\text{O} + \text{CO}. \tag{2}$$

This assumption is supported by the observation that HNCO reduces NO, e.g., in diesel exhaust, at temperatures above 400 °C. Acke et al. have shown by isotope-labeling transient experiments that isocyanates adsorbed on Pt supported on Al_2O_3 reduce NO to N_2 and N_2O [37]. Schießer et al. have demonstrated by IR spectroscopy a correlation between the intensity of the –NCO band on Pt–Al-MCM-41 and the conversion of NO [38]. Similarly to the materials discussed here, the isocyanates detected were mainly adsorbed on anionic defect sites of the Al_2O_3-containing support material. Interestingly, we have observed the formation of –NCO and N_2O in the absence of a noble metal, indicating that metal clusters are not a prerequisite for the reaction of NO with isocyanate intermediates at elevated temperatures (above 500 °C). N_2O is a common by-product in the reaction of NO with CO over noble metal-impregnated oxides. The formation of N_2O was already observed over mixed oxide materials, such as nonstoichiometric nickel–copper spinel manganites and Al-MCM-41 impregnated with Pt [35,38]. For MCM-36-type materials with alkaline earth aluminum oxide pillars significantly higher yields of N_2O were observed compared to the nonpillared parent material MCM-22, indicating that the basic mixed oxide phases enhance the N_2O formation. The generation of N_2O is favored by low oxygen concentrations and higher concentrations of Mg and Ba (cf. Fig. 5). While the yield of N_2 increased continuously with temperature, the yield of N_2O reached a maximum between 575 and 675 °C, which indicates the decomposition of N_2O,

$$\text{N}_2\text{O} \rightarrow \text{N}_2 + \tfrac{1}{2}\text{O}_2, \tag{3}$$

over the oxide pillars in the interlayer galleries. It is well known that at temperatures above 400 °C N_2O decomposes over basic oxides such as MgO, CaO, and BaO (cf. Refs. [39–42] and references therein).

In the presence of excess oxygen (cf. Fig. 4b) significantly lower yields of N_2O were found for all materials investigated. In general, higher oxygen concentrations decrease the availability of the reductant CO and additionally favor the oxidation of N_2O to NO and NO_2, inhibiting the deNO_x reaction. Interestingly, under oxygen-deficient reaction conditions the maximum of the N_2O formation occurs over MgO-containing pillared zeolites at lower temperatures compared to the more basic $BaO–Al_2O_3$-MCM-36 and $BaO–Al_2O_3–SiO_2$-MCM-36 materials, which could result from a higher coverage of basic sites with nitrate and carbonate species, thus inhibiting the N_2O decomposition.

Hori et al. have shown that N_2O can also be easily reduced over MgO by adsorbed formate species. The interaction of CO with basic hydroxyl groups of MgO leads to formates which subsequently reduce N_2O to N_2 [31],

$$\text{Mg(OH)}_2 + \text{CO} \xrightarrow{\text{MgO}} (\text{MgOH})^+ \text{H–C}(=\text{O})\text{O}^-, \tag{4}$$

$$(\text{MgOH})^+ \text{H–C}(=\text{O})\text{O}^- + \text{N}_2\text{O} \xrightarrow{\text{MgO}} \text{CO}_2 + \text{N}_2 + \text{Mg(OH)}_2. \tag{5}$$

At temperatures below 500 °C formates were observed on $MgO–Al_2O_3$-MCM-36 during the reaction of CO with nitrites and nitrates adsorbed on the catalyst surface, as indicated by characteristic IR bands at 2930, 1610, and 1384 cm^{-1}. However, it is speculated that at elevated temperatures typical of the FCC process decomposition of nitrous oxide over the oxide pillars is the dominating reaction.

Generally, the higher catalytic activity of $MgO–Al_2O_3$-MCM-36 at lower temperatures is attributed to an increased resistance to poisoning by CO_2, which is a major reaction product. MCM-36 materials with the more basic BaO pillars will be more easily deactivated by the formation of carbonates than the MgO-containing MCM-36 materials. Consequently, the reduction of NO by CO over MCM-36-type materials might be explained as a two-step process involving the formation of nitrous oxide as an intermediate

$$2\text{NO} + \text{CO} \rightarrow \text{N}_2\text{O} + \text{CO}_2, \tag{6}$$

$$\text{N}_2\text{O} + \text{CO} \rightarrow \text{N}_2 + \text{CO}_2, \tag{7}$$

$$2\text{NO} + 2\text{CO} \rightarrow \text{N}_2 + 2\text{CO}_2. \tag{8}$$

Reaction (7) corresponds to the decomposition of nitrous oxide and is generally considered as a fast process compared to reaction (6) [35]. A detailed discussion of the kinetics of N_2O decomposition on oxide catalysts can be found in [43].

In the absence of water, all derivatives of MCM-36 show stable catalytic activity in time-on-stream measurements, indicating that the composite structure is stable during the high-temperature reactions. In the presence of water, however, the catalytic activity for the reduction of NO with CO decreased after ∼ 5.5 h (see Fig. 5), which is attributed to a gradual dealumination of the nanocomposite materials during the high-temperature reaction in the presence of 5% H_2O.

4.2. Comparison of lab-scale reactor and pilot plant kinetic measurements

Under reaction conditions similar to those found in the regenerator unit of a FCC plant, additives based on MCM-36-type catalysts with mixed $MgO–Al_2O_3$ and $BaO–Al_2O_3$ oxide pillars are only active in the oxygen-deficient region of the fluidized bed, where most of the oxygen is consumed by burning off the coke present on the catalyst. After reaction at 500–575 °C for 5–10 h, high water concentrations (5–8%) found in parts of the regenerator and the stripper have a negative effect on the catalytic activity of the materials, probably due to steam-induced dealumination reactions as suggested by ^{27}Al MAS-NMR (spectra not shown). The performance of the MCM-36-type additives under reaction conditions typical for a fluidized-bed reactor used for the regeneration of coked FCC catalysts indicated that the oxidative regeneration of carbonaceous deposits on the spent catalysts leads to O_2, N_2, CO, CO_2, H_2O, SO_x, and NO_x formation in the flue gas of the regenerator (see Table 3 and Fig. 11) [6,27,44]. Additionally, NH_3 and HCN are found in lower concentrations (10–200 ppm) as reduced nitrogen-containing intermediates of coke pyrolysis and precursors of NO_x [8,14,27]. Performing the regeneration experiment in the presence of CP-3, a commercial Pt-based CO combustion promoter, leads to a decrease of CO formation accompanied by a significant increase in NO_x emissions by ∼ 300%. As shown earlier by Yaluris et al. and our group this observation can be attributed to the Pt-catalyzed oxidation of HCN and NH_3 to NO_x comparable to the Ostwald process [8,14,27]. In contrast, the pillared MCM-36 materials based on MCM-22 zeolites yielded a reduction of NO emissions, while only a very small conversion of CO was observed. The regeneration experiments showed the typical sequential burning of coke species from the deactivated catalyst. As can be seen from the oxidative regeneration (see Fig. 11) NO is mainly formed at the end of the regeneration experiment, when most of the carbon has been burnt off. All additives led to a reduction of NO emissions in this temperature range, $BaO–Al_2O_3$-MCM-36 being the most active. The decrease of NO emissions was accompanied by a distinct removal of CO in the region of the second maximum of CO formation (cf. Fig. 11), which strongly suggests a reduction of NO with CO. The relatively low conversions of NO can be best explained with a significantly lower concentration of CO at the end of the experiment and are in line with observations of Efthimiadis et al. for other FCC deNO_x additives [28]. The conversion of NO in the regeneration experiment in the fluidized-bed reactor is slightly lower than in the fixed-bed catalytic experiments in the excess of oxygen (Fig. 1b). All particles in the fluidized bed (CSTR reactor) show the same extent of regeneration, which implies that in the beginning of regeneration CO is primarily formed, while NO is emitted when the regeneration has proceeded. Consequently, at this stage of regeneration high O_2 (1.5–2%) and low CO concentrations (< 0.1%) are encountered in the fluidized bed. Under realistic conditions in a continuously operated industrial FCC regenerator, lower oxygen and nearly constant carbon monoxide concentrations are present in the oxygen-depleted zone of the fluidized bed, which should most probably lead to higher NO conversions. Nevertheless, the MCM-36-type additives reduce NO even in the presence of very low CO concentrations, indicating the presence of a second reduction mechanism.

During the regeneration of the FCC catalysts HCN and NH_3 are present especially in the oxygen-depleted zones of the fluidized bed. At temperatures above 700 °C HCN is hydrolyzed to NH_3 over basic oxides such as the mixed oxide clusters of the pillared zeolites [45],

$$HCN + H_2O \rightarrow NH_3 + CO, \tag{9}$$

which reduces NO over Brønsted acid sites found in the zeolite layers of the composite materials [46]:

$$3NO + 2NH_3 \rightarrow 2.5N_2 + 3H_2O. \tag{10}$$

Various studies claim that NH_3 bonded to Brønsted acid sites of H-form zeolites reacts with NO_2-type intermediates formed on the zeolite surface during selective catalytic reduction (SCR) reactions ([46] and references therein).

MCM-36 derivatives with mixed alkaline earth–aluminum oxide pillars allow stabilization of reactive nitrogen-containing intermediates such as NH_3 (on the Brønsted and strong Lewis acid sites), HCN (by basic oxide-catalyzed hydrolysis to NH_3), and NO_x (formation of nitrite and nitrate species on the mixed oxide pillars) prior to the SCR reaction to N_2, which probably occurs on Brønsted acid sites of the MCM-22 zeolite layers. Consequently, the potential of MCM-36-type additives for the reduction of NO emissions during the regeneration of FCC catalysts may be attributed to catalytic active sites for (i) the reduction of NO with CO and (ii) for the reduction of NO with NH_3.

In contrast to the catalytic experiments in the fixed-bed reactor, in the fluidized-bed reactor the best results were obtained for the BaO-containing nanocomposite materials. The higher catalytic activity of such pillared zeolites is tentatively explained by an enhanced reactivity for the hydrolysis of the reaction intermediate HCN to NH_3 over the $BaO–Al_2O_3$ pillars [Eq. (9)]. This reaction provides a higher concentration of NH_3, which can act as a reducing agent in the reaction with NO. In contrast to the fixed-bed experiments deactivation by poisoning with carbonate species does not seem to play an important role probably due to the lower CO_2 concentrations in our regeneration experiments.

From a practical point of view it is important to note that the MCM-36-type additives can be used together with a Pt-based CO combustion promoter (Table 4). Compared to the pure spent catalyst (base case) the NO emissions have increased due to the oxidation of reduced nitrogen containing intermediates by the noble metal-containing CO promoter. However, in comparison with sole CP-3 lower NO concentrations were measured, when the additives were used additionally in the regeneration experiment. As the promoter significantly lowers the concentration of CO in the regeneration experiment, the reduction of NO emissions is best explained with a direct interaction of the MCM-36 catalysts with the precursor molecules (NH_3, HCN) for the formation of NO_x. As outlined above, Pt-based CO combustion promoters lead to the oxidation of HCN and NH_3, which are formed during the pyrolysis of nitrogen-containing coke molecules. It is speculated that the (intermediate) NH_3 is temporarily trapped on Brønsted acid sites in the zeolite layers or on strong Lewis acid sites in the mixed oxide pillars, thus preventing an immediate oxidation to NO over the Pt catalyst. This hypothesis is supported from the fact that $MgO–Al_2O_3–SiO_2$-MCM-36 and $BaO–Al_2O_3$-SiO_2-MCM-36 showed the highest catalytic activity for the reduction of NO in the presence of CP-3, although the concentration of Mg and Ba is lower than in the other materials. We have shown earlier by temperature-programmed oxidation of NH_3 that both materials possess additional, strong Brønsted acid sites on the pillars close to the basic mixed oxide clusters [23]. Consequently, NH_3 adsorbed on the acid sites can react immediately with NO_x (from the gas phase or adsorbed on the basic oxide pillars) to N_2. The combination of a conventional Pt-based CO promoter and MCM-36 derivatives allows the simultaneous control of CO and NO emissions in the FCC regenerator (see Table 4). A further reduction of NO emissions might be achieved by a variation of the concentration of additive in the inventory and a continuous operation mode of the fluidized-bed reactor, which should better simulate the actual situation in the FCC regenerator.

5. Conclusions

MCM-36-type additives with mixed alkaline earth aluminum oxide ($MgO–Al_2O_3$-MCM-36, $BaO–Al_2O_3$-MCM-36, $MgO–Al_2O_3–SiO_2$-MCM-36, $BaO–Al_2O_3–SiO_2$-MCM-36) pillars are highly active additives for the reduction of NO with CO under reaction conditions similar to the oxygen-depleted zone of the FCC regenerator. The reaction proceeds via nitrite, nitrate, and isocyanate intermediates, which are adsorbed on the basic mixed oxide clusters in the interlayer galleries of the MCM-36-type materials. N_2 and N_2O are formed by the reaction of isocyanates with NO. At temperatures characteristic of the FCC regeneration process N_2O decomposes over basic oxide clusters in the composite materials yielding N_2. The reduction of NO by CO over MCM-36-type materials can be explained by a two-step process involving the formation of nitrous oxide as an intermediate. In the presence of H_2O the catalytic activity decreases due to a gradual dealumination of the composite material during the high-temperature reaction. The additives show a reduction of NO_x emissions even in experiments simulating the regeneration of industrial coked FCC catalysts in a fluidized-bed reactor. In contrast to Pt-based additives, the nanocomposite materials do not oxidize reduced nitrogen containing intermediates (NH_3, HCN), which are generated during the pyrolysis of nitrogen coke species, but lower the concentration of NO_x released in the flue gases. It is speculated that during the regeneration of spent FCC catalysts the MCM-36-type additives catalyze, in addition to the NO + CO reaction, the SCR reaction of NO with NH_3 to N_2 on Brønsted acid sites in the zeolite layers or on the pillars in the interlayer galleries. HCN, which is a key intermediate in the nitrogen chemistry of the FCC unit, might be hydrolyzed to NH_3 over the basic oxide pillars in the interlayer galleries. The additives can be used in combination with Pt-based CO promoters to simultaneously control the level of NO *and* CO in the regeneration unit.

Acknowledgments

Financial support of the European Union (Project G1RD-CT99-0065-“DENOXPRO”) is gratefully acknowledged. The authors thank Dr. H. Rhemann (OMV), Dr. R. Harding, Dr. J. Nee, and Dr. G. McElhiney (GRACE-Davison) for helpful discussions concerning FCC deNO_x technologies.

References

[1] R.H. Harding, A.W. Peters, J.R.D. Nee, Appl. Catal. A 221 (2001) 389.
[2] J.-O. Barth, Erdöl Erdgas Kohle 119 (2003) 86.
[3] W.-C. Cheng, G. Kim, A.W. Peters, X. Zhao, K. Rajagopalan, M.S. Ziebarth, C.J. Pereira, Catal. Rev.-Sci. Eng. 40 (1998) 39.
[4] R. Mann, Catal. Today 18 (1993) 509.
[5] A.W. Peters, G. Yaluris, G.W. Weatherbee, X. Zhao, Fluid Crack. Catal. (1998) 259.
[6] X. Zhao, A.W. Peters, G.W. Weatherbee, Ind. Eng. Chem. Res. 36 (1997) 4535.
[7] D.A. Cooper, A. Emanuelsson, Energ. Fuel. 6 (1992) 172.
[8] J.-O. Barth, A. Jentys, J.A. Lercher, in: Proceedings of the 17th World Petroleum Congress, Rio de Janeiro, 2002, vol. 3, Institute of Petroleum, London, 2003, p. 445.
[9] E.F. Iliopoulou, E.A. Efthimiadis, I.A. Vasalos, J.-O. Barth, J.A. Lercher, Appl. Catal. B 47 (2004) 165.
[10] E.A. Efthimiadis, A.A. Lappas, D.K. Iatrides, I.A. Vasalos, Ind. Eng. Chem. Res. 40 (2001) 515.
[11] B. Wen, M. He, Appl. Catal. B 37 (2002) 75.
[12] B. Wen, M. He, C. Costello, Energ. Fuel. 16 (2002) 1048.
[13] A. Corma, A.E. Palomares, F. Rey, F. Márquez, J. Catal. 170 (1997) 140.
[14] J.-O. Barth, A. Jentys, J.A. Lercher, Ind. Eng. Chem. Res. 43 (2004) 2368.

[15] J.-O. Barth, A. Jentys, J.A. Lercher, Ind. Eng. Chem. Res. 43 (2004) 3097.
[16] D.O. Chessmore, C.E. Rudy Jr., US patent 4,199,435, 1999.
[17] W.J. Roth, C.T. Kresge, J.C. Vartuli, M.E. Leonowicz, A.S. Fung, S.B. McCullen, Stud. Surf. Sci. Catal. 94 (1995) 301.
[18] W.J. Roth, J.C. Vartuli, C.T. Kresge, Stud. Surf. Sci. Catal. 129 (2000) 501.
[19] Y.J. He, G.S. Nivarthy, F. Eder, K. Seshan, J.A. Lercher, Micropor. Mesopor. Mater. 25 (1998) 207.
[20] W. Roth, Jerzy, J. Vartuli, Clarke, Stud. Surf. Sci. Catal. 141 (2002) 273.
[21] J.-O. Barth, J. Kornatowski, J.A. Lercher, J. Mater. Chem. 12 (2002) 369.
[22] S. Xie, M.P. Rosynek, J.H. Lunsford, J. Catal. 188 (1999) 24.
[23] J.O. Barth, A. Jentys, J. Kornatowski, J.A. Lercher, Chem. Mater. 16 (4) (2004) 724.
[24] J.-O. Barth, R. Schenkel, J. Kornatowski, J.A. Lercher, Stud. Surf. Sci. Catal. 135 (2001) 136.
[25] L. Rheaume, R.E. Ritter, J.J. Blazek, I.A. Montgomery, Oil Gas J. 74 (1976) 103.
[26] K. Limbach, S. Tamhankar, S. Ganguly, V. Balse, R. Menon, R. Ramachandran, Petroleum Technology Quaterly—eptq.com—The Refining, Gas and Petrochemical Processing Website, http://www.eptq.com/, 2000.
[27] G. Yaluris, A.W. Peters, in: 2nd Int. Conf. on Refining Processes, AIChE Spring National Meeting, Houston, 1999, p. 27.
[28] E.A. Efthimiadis, E.F. Iliopoulou, A.A. Lappas, D.K. Iatrides, I.A. Vasalos, Ind. Eng. Chem. Res. 41 (2002) 5401.
[29] K.I. Hadjiivanov, Catal. Rev.-Sci. Eng. 42 (2000) 71.
[30] B. Westerberg, E. Fridell, J. Mol. Catal. A 165 (2001) 249.
[31] B. Hori, N. Takezawa, Catal. Lett. 12 (1992) 383.
[32] V.A. Matyshak, O.V. Krylov, Catal. Today 25 (1995) 1.
[33] K.L. Dishman, P.K. Doolin, L.D. Tullock, Ind. Eng. Chem. Res. 37 (1998) 4631.
[34] M. Shelef, K. Otto, H. Gandhi, J. Catal. 12 (1968) 361.
[35] C. Drouet, P. Alphonse, A. Rousset, Appl. Catal. B 33 (2001) 35.
[36] H. Knözinger, P. Ratnasamy, Catal. Rev.-Sci. Eng. 17 (1978) 31.
[37] F. Acke, B. Westerberg, M. Skoglundh, J. Catal. 179 (1998) 528.
[38] W. Schiesser, H. Vinek, A. Jentys, Appl. Catal. B 33 (2001) 263.
[39] S. Xie, J.H. Lunsford, Appl. Catal. A 188 (1999) 137.
[40] E.M. Serwicka, Polish J. Chem. 75 (2001) 307.
[41] M.A. Wójtowicz, J.R. Pels, J.A. Moulijn, Fuel Process. Technol. 34 (1993) 1.
[42] F. Kapteijn, J. Rodriguez-Mirasol, J.A. Moulijn, Appl. Catal. B 9 (1996) 25.
[43] E.R.S. Winter, J. Chem. Soc. A (1968) 2889.
[44] G. Yaluris, A.W. Peters, in: J.G. Reynolds, M.R. Khan (Eds.), Designing Transportation Fuels for a Cleaner Environment, Taylor & Francis, Philadelphia, 1999, p. 151.
[45] S. Schäfer, B. Bonn, Chem. Ing. Techn. 71 (1999) 613.
[46] J. Eng, C.H. Bartholomew, J. Catal. 171 (1997) 27.